TELKOMNIKA Indonesian Journal of Electrical Engineering
Vol.12, No.2, February 2014, pp. 1060 ~ 1067
DOI: http://dx.doi.org/10.11591/telkomnika.v12i2.4328

Unstable Manifold of Hénon Map

LI Zhongqin, JIA Meng*
Department of Electrical Engineering, XinXiang University
East Jin Sui street, XinXiang city, HeNan province, China
*Corresponding author, e-mail: tianshi_cd@163.com

Abstract

A new algorithm is presented for computing one dimensional unstable manifold of a map and Hénon map is taken as an example to test the performance of the algorithm. The unstable manifold is grown with new point added at each step and the distance between consecutive points is adjusted according to the local curvature. It is proved that the gradient of the manifold at the new point can be predicted by the known points on the manifold and in this way the preimage of the new point could be located immediately. During the simulation, it is found that the unstable manifold of Hénon map coincides with its direct iteration when canonical parameters are chosen which means order is obtained out of chaos. In the other several groups of parameters the two branches of the unstable manifolds are nearly symmetric, and they serve as the borderline of the Hénon map iteration sequence. We hope that this would contribute to the further exploration of Hénon map.

Keywords: *discrete dynamical system, hyperbolic fixed point, unstable manifold*

1. Introduction

Dynamical system can simply be classified into two categories: continuous dynamical system and discrete dynamical system. And discrete dynamical system often takes the form of iterated functions. Various examples in applications can be depicted by iterated functions, and Hénon map [1] is one of the most famous ones. Hénon map is chaotic for canonical parameters and it is also widely used in Image Encrypting [2], fractal science, etc. Hénon map takes the form as:

$$\begin{cases} x_{n+1} = 1 - ax_n^2 + by_n \\ y_{n+1} = x_n \end{cases} \quad (1)$$

It can also be written as:

$$G\begin{pmatrix} x \\ y \end{pmatrix} = \begin{pmatrix} 1 - ax^2 + by \\ x \end{pmatrix} \quad (2)$$

a and b are free parameters. For canonical parameters $a = 1.4 \quad b = 0.3$, the system is chaotic. Let's consider the second iterate of G.

$$F = G^2\begin{pmatrix} x \\ y \end{pmatrix} = \begin{pmatrix} 1 - a(1 - ax^2 + by)^2 + bx \\ 1 - ax^2 + by \end{pmatrix} \quad (3)$$

In the next section some basic concepts about stable and unstable manifold are introduced.

Received August 4, 2013; Revised September 7, 2013; Accepted October 8, 2013

2. Mathematical Setting

Suppose $F: R^n \to R^n$ is an orientation preserving diffeomorphism.

$$x_{m+1} = F(x_m) \tag{4}$$

If x_0 is a starting point, then,

$$F^{k+l}(x_0) = F^k(F^l(x_0)) \tag{5}$$

k and l are integers. If $x_0 \in R^n$ meets the condition $F(x_0) = x_0$, then x_0 is a fixed point of F. From (5) we know x_0 is also a fixed point of F^k. Consider the Jacobian matrix $A = DF(x_0) = [\partial F_i / \partial x_j](x_0)$ of F at x_0. x_0 is hyperbolic if the modulus of eigenvalues of A is different from 1. The eigenvalues whose modulus is smaller than 1 are called stable and their corresponding eigenvectors $\{v_1, v_2, \cdots, v_l\}$ span the stable eigenspace E^s. The other eigenvalues whose modulus is bigger than 1 are called unstable and their corresponding eigenvectors $\{v_{l+1}, v_{l+2}, \cdots, v_n\}$ span the unstable eigenspace E^u.

Theorem 1. Suppose $F: R^n \to R^n$ is an orientation preserving diffeomorphism and x_0 is a fixed point of F, then in the neighborhood U of x_0, there exists local stable and unstable manifolds.

$$W^s_{loc}(x_0) = \{x \in U : \lim_{k \to +\infty} F^k(x) \to x_0\} \tag{6}$$

$$W^u_{loc}(x_0) = \{x \in U : \lim_{k \to -\infty} F^k(x) \to x_0\} \tag{7}$$

E^s and E^u are tangent to $W^s_{loc}(x_0)$ and $W^u_{loc}(x_0)$ at x_0 respectively.

See reference [3] for more information. Global stable and unstable manifold are defined as:

$$W^s(x_0) = \{x \in R^n : \lim_{k \to +\infty} F^k(x) \to x_0\} = \bigcup_{i=0}^{-\infty} F^i(W^s_{loc}(x_0)) \tag{8}$$

$$W^u(x_0) = \{x \in R^n : \lim_{k \to -\infty} F^k(x) \to x_0\} = \bigcup_{i=0}^{+\infty} F^i(W^u_{loc}(x_0)) \tag{9}$$

It's clear that the global manifold is the image of the local manifold.

Stable and unstable manifolds play an important role in analyzing the dynamics of a given system. They form basins of attraction between different attractors, and complexed dynamics like chaos, homoclinic and heteroclinic would occur when they intersect. Computation of stable and unstable manifolds will contribute to the further study of all these fields.

Several algorithms [4-11] have come up. The algorithms [7, 8] use the idea of growing the unstable manifold and one point is found and added at a prespecified distance away from a given point each step. They have to search along the known segment on the unstable manifold back and forth to find the preimage of the new point, and it is the choke point which reduces the efficiency of the algorithm. It is verified in this paper that the gradient of the unstable manifold can be predicted by the known points on the unstable manifold and the scheme can be used to locate the preimage of the new point quickly.

3. Gradient Prediction

According to the definition (9) of global unstable manifold, we know if $x \in W^u(x_0)$ then $F(x) \in W^u(x_0)$. Expand F at x as Taylor series. $F(x+£_i) = F(x) + F'(x)£_i + o(\|£_i\|)$

Ignore the high order terms $F(x+£_i) = F(x) + F'(x)£_i = F(x) + \mathbf{A}\boldsymbol{\varepsilon}_i$

$\mathbf{A} = \mathbf{D}F(x) = \left[\dfrac{\partial F_i}{\partial x_j}\right](x)$ is the Jacobian matrix of F at x.

As shown in Fig.1, for 2D phase space

$$\boldsymbol{\varepsilon}_i = \begin{bmatrix} \Delta x \\ \Delta y \end{bmatrix} \tag{10}$$

Then

$$\mathbf{E} = F(x+£_i) - F(x) = \mathbf{A}\boldsymbol{\varepsilon}_i = \begin{bmatrix} \dfrac{\partial F_1}{\partial x} & \dfrac{\partial F_1}{\partial y} \\ \dfrac{\partial F_2}{\partial x} & \dfrac{\partial F_2}{\partial y} \end{bmatrix} \begin{bmatrix} \Delta x \\ \Delta y \end{bmatrix} = \begin{bmatrix} \dfrac{\partial F_1}{\partial x}\Delta x + \dfrac{\partial F_1}{\partial y}\Delta y \\ \dfrac{\partial F_2}{\partial x}\Delta x + \dfrac{\partial F_2}{\partial y}\Delta y \end{bmatrix} = \begin{bmatrix} \Delta x' \\ \Delta y' \end{bmatrix} = \boldsymbol{\varepsilon}_i' \tag{11}$$

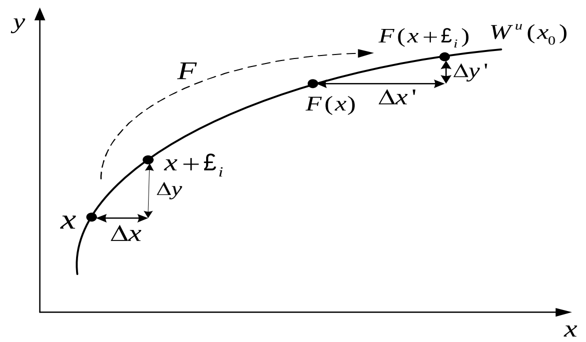

Figure 1. Gradient prediction

When $£_i \to 0$, it follows $x+£_i \to x$ and $F(x+£_i) \to F(x)$. So $\Delta x / \Delta y$ can be taken as the gradient of the unstable manifold at x while $\Delta x' / \Delta y'$ is the gradient at $F(x)$.

During the computation, x, $x+£_i$ and $F(x)$ are known points on the unstable manifold and $F(x+£_i)$ is unknown. The unknown gradient of $W^u(x_0)$ at $F(x)$ can be approximated by known points x and $x+£_i$. And that is why we call our algorithm gradient prediction.

4. The algorithm

Evaluate the Jacobian matrix of F at the hyperbolic fixed point x_0 and take a point p_0 at a distance of ¢ away from x_0 along the unstable eigenvector. When ¢ is chosen small enough, the segment between x_0 and p_0 could be a good approximation of $W^u_{loc}(x_0)$. The image of p_0 is $p_1 = F(p_0)$. Put x_0, p_0 and p_1 in the ordered sequence $M = \{x_0, p_0, p_1\}$.

The algorithm adds one point to M per step. Suppose $M = \{x_0, p_0, p_1, \cdots, p_k\}$ and the preimage of p_k is p_k'. Note that p_k' does not necessarily belong to M, it is the interpolation of the points that belong to M most of the time. If we connect the successive points in M and denote the new set as M', then $p_k' \in M'$. Assume p_k' lies on the segment with endpoints p_i and p_{i+1}. The gradient at p_k' can be approximated by the gradient of segment $p_i p_{i+1}$.

Suppose we want to add a new point p_{k+1} at a distance of Δ_k from p_k. It can be done in the following two steps,

1) Prediction: $p_{i+1} - p_k'$ is chosen as an initial guess for $£_i$. Then $£_i' = A£_i$ and the modulus of $£_i'$ is $\Delta_k' = \| £_i' \| = \sqrt{(\Delta x')^2 + (\Delta y')^2}$.

2) Correction: The ratio between Δ_k' and the expectation Δ_k is $R = \Delta_k / \Delta_k'$, then $£_i$ is adjusted by $£_i = R * £_i$. Because $£_i$ and $£_i'$ are linearly related so that Δ_k' will be of the same modulus with Δ_k after the adjustment.

Here the gradient prediction is used to approximate Δ_k'.

Now $p_{k+1}' = p_k' + £_i$ is a good approximation of the preimage of p_{k+1}. If p_{k+1}' exceeds the segment $p_i p_{i+1}$, it is necessary to switch to the next segment in M'. p_{k+1}' is mapped to get the exact position of p_{k+1} and the difference between $p_{k+1} = F(p_{k+1}')$ and $p_k + £_i'$ is negligible. Now it is necessary to check if Δ_k is acceptable and the strategy [6, 7] is used.

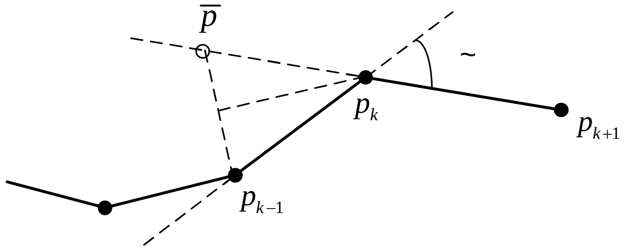

Figure 2. Curvature constraint

As is exhibited in Figure 2

$$\sin\left(\frac{\sim}{2}\right) = \frac{\| \bar{\vec{\mathbf{p}}} - \overrightarrow{\mathbf{p_{k-1}}} \|}{2 \| \overrightarrow{\mathbf{p_k}} - \overrightarrow{\mathbf{p_{k-1}}} \|} \tag{12}$$

Where

$$\bar{\vec{\mathbf{p}}} = \overrightarrow{\mathbf{p_k}} + \frac{\| (\overrightarrow{\mathbf{p_k}} - \overrightarrow{\mathbf{p_{k-1}}}) \|}{\| (\overrightarrow{\mathbf{p_k}} - \overrightarrow{\mathbf{p_{k+1}}}) \|} (\overrightarrow{\mathbf{p_k}} - \overrightarrow{\mathbf{p_{k+1}}}) \tag{13}$$

$\bar{p}$ lies on the line through p_k and p_{k+1} with the property $\| \bar{\vec{\mathbf{p}}} - \overrightarrow{\mathbf{p_k}} \| = \| \overrightarrow{\mathbf{p_{k-1}}} - \overrightarrow{\mathbf{p_k}} \|$. If $\sim$ is small enough, $\sin(\sim/2) \approx \sim/2$, then formula (12) can be simplified as

$$\sim = \frac{\| \bar{\vec{\mathbf{p}}} - \overrightarrow{\mathbf{p_{k-1}}} \|}{\| \overrightarrow{\mathbf{p_k}} - \overrightarrow{\mathbf{p_{k-1}}} \|} \tag{14}$$

$\sim$ should satisfy the following condition

$$\sim_{min} < \sim < \sim_{max}$$
$$(\Delta\sim)_{min} < \Delta_k \sim < (\Delta\sim)_{max} \quad (15)$$

Where $\Delta_k = \| \overrightarrow{\mathbf{p_{k+1}}} - \overrightarrow{\mathbf{p_k}} \|$. The first condition keeps $\sim$ small to avoid missing details of the unstable manifold, and the second condition controls the local interpolation error. The new point p_{k+1} is accepted if both $\sim < \sim_{max}$ and $\Delta_k \sim < (\Delta\sim)_{max}$. At the same time, if $\Delta_k < \Delta_{min}$ (Δ_{min} is the minimum distance between successive points), p_{k+1} is accepted too. When both $\sim < \sim_{min}$ and $\Delta_k \sim < (\Delta\sim)_{min}$, we'll need to set $\Delta_{k+1} = 2\Delta_k$. If any of the condition in (15) is not satisfied, we have to replace Δ_k with $\Delta_k / 2$ and recompute p_{k+1}.

Add p_{k+1} to the ordered sequence M and continue the computation until the arc length of M' reaches the desired arc length ARC.

After all of the aforementioned steps are finished, one branch of $W^u(x_0)$ is computed and we need to start over the computation on the opposite direction of the unstable eigenvector of A to get the other branch of $W^u(x_0)$. $W^u(x_0)$ is the composition of the two branches.

5. Unstable manifold of Hénon map

The following parameters were used in the paper: $¢ = 0.001$, $\sim_{max} = 0.3$, $\sim_{min} = 0.2$, $\Delta_{max} = 0.001$, $\Delta_{min} = 0.0001$, $(\Delta\sim)_{max} = 10^{-4}$, $(\Delta\sim)_{min} = 10^{-5}$.

By solving the equation $G(x, y) = (x, y)$, it is easy to know that

$$x_0 = (x, y) = \left(\left[(b-1) + \sqrt{(b-1)^2 + 4a} \right] \Big/ 2a, \left[(b-1) + \sqrt{(b-1)^2 + 4a} \right] \Big/ 2a \right) \quad (16)$$

is a fixed point of Hénon map G. And x_0 is also a fixed point of $F = G^2$. a and b should satisfy $(b-1)^2 + 4a \geq 0$ to make sure that both x and y are real.

The Jacobian matrix of F at x_0 is

$$\mathbf{A} = \mathbf{D}F(x_0) = [\partial F_i / \partial x_j](x_0) = \begin{bmatrix} 2a^2(1 - ax^2 + by) + b & -2ab(1 - ax^2 + by) \\ -2ax & b \end{bmatrix}_{x_0} \quad (17)$$

1) When $a = 1.4$, $b = 0.3$, the fixed point is $x_0 = (0.6314, 0.6314)$. The Jacobian matrix of F at x_0 is $\mathbf{A} = \begin{bmatrix} 3.4251 & -0.5303 \\ -1.7678 & 0.3 \end{bmatrix}$. $\det(\mathbf{A}) = \det(\mathbf{D}F(x_0)) > 0$, so F is orientation preserving. $\mathbf{A}$ has two eigenvalues $\text{a}_u = 3.7008$ and $\text{a}_s = 0.0243$. The unstable manifold of hyperbolic fixed point x_0 is shown in Fig.3. The arc lengths of the two branches are both $ARC = 50$.

It is easy to see from Fig.3 that the distribution of points of unstable manifold is almost the same with that of Hénon map iteration sequence and the difference is the sequence of points in (a) is ordered while points in (c) is unordered. To show this, we connect the first 20 points in (c) and plot it in (d). It's very clear that the points are unordered. That is to say, we obtain order out of chaos.

2) When $a = 0.2$, $b = 0.99$, the fixed point is $x_0 = (2.2112, 2.2112)$. The Jacobian matrix of F at x_0 is $\mathbf{A} = \begin{bmatrix} 1.7723 & -0.8756 \\ -0.8845 & 0.99 \end{bmatrix}$, with eigenvalues $\text{a}_u = 2.3442$ and $\text{a}_s = 0.4181$.

$\det(A) = \det(DF(x_0)) > 0$. The unstable manifold of hyperbolic fixed point x_0 is shown in Fig.4. The arc lengths of the two branches are both $ARC = 70$.

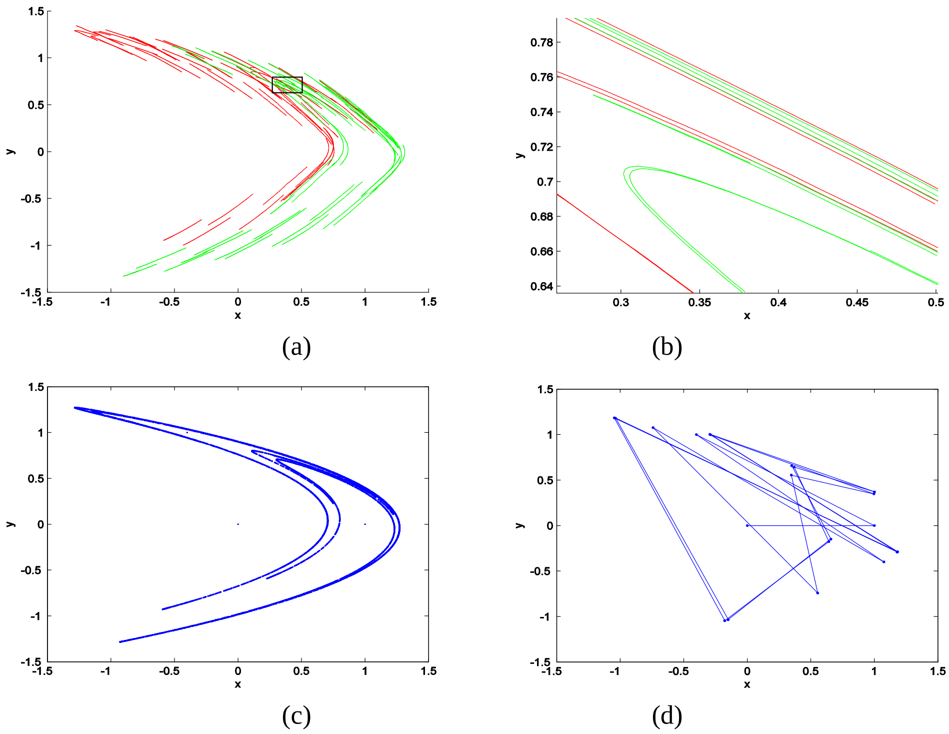

Figure 3. (a)Unstable manifold (b)An enlargement of the manifold (c) Hénon map iteration sequence starting at (0,0) with 10,000 iterations (d)Connect the first 20 points in (c)

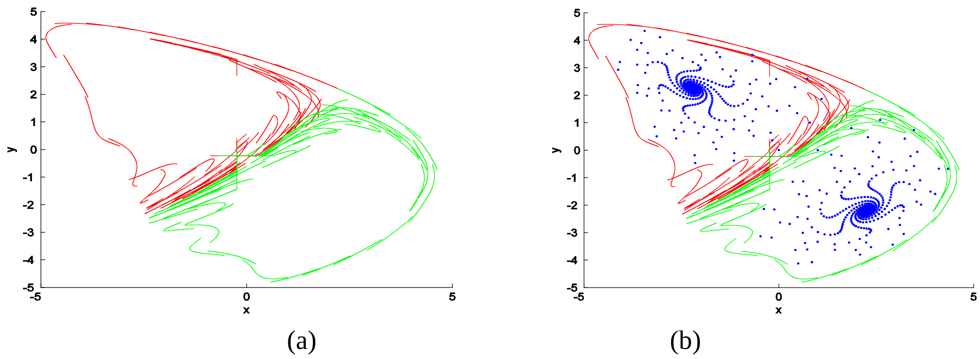

Figure 4. (a) Unstable manifold (b) Unstable manifold and the Hénon map iteration sequence

We can see from Fig.4 that the unstable manifold tends to accumulate inside, at the same time, it serves as the boundary which keeps the Hénon map iteration sequence (starting at (0,0) with 10,000 iterations) inside. When $a = 0.2$, $b = 0.96$ and $a = 0.2$, $b = 0.98$, the situation is similar.

3) when $a = 0.2$, $b = 0.9991$ the fixed point is $x_0 = (2.2338, 2.2338)$. The Jacobian matrix of F at x_0 is $\mathbf{A} = \begin{bmatrix} 1.7975 & -0.8927 \\ -0.8935 & 0.9991 \end{bmatrix}$, with eigenvalues $a_u = 2.3766$ and $a_s = 0.42$.

$\det(\mathbf{A}) = \det(\mathbf{D}F(x_0)) > 0$. The unstable manifold of hyperbolic fixed point x_0 is shown in Fig.5. The arc lengths of the two branches are both $ARC = 50$.

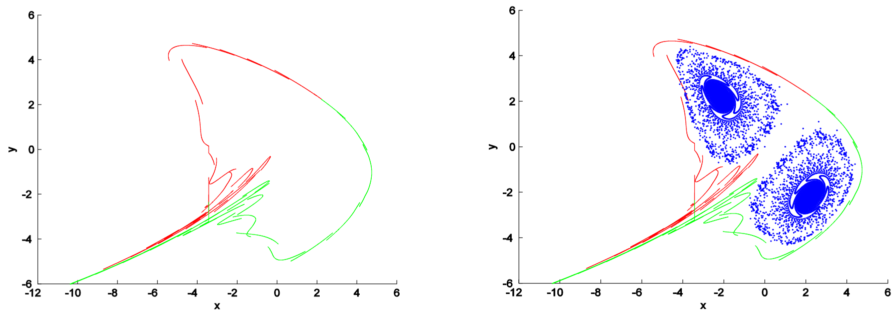

(a) (b)

Figure 5. (a) Unstable manifold (b) Unstable manifold and the Hénon map iteration sequence

Compared to Fig.4, the unstable manifold in Fig.5 begins to "walk" outward. From Fig.5 (b) we know the Hénon map iteration sequence (starting at (0,0) with 10,000 iterations) is still surrounded by the unstable manifold.

5. Conclusion

A new algorithm is put forward for computing the one dimensional unstable manifold of a map. The algorithm grows the manifold with one point added each step. And the distance between consecutive points are adjusted according to the local curvature and distance constraint. The preimage of the newly added point is located quickly with a gradient prediction scheme and this is the main advantage over the algorithm proposed in reference [7]. Rather than using bisection algorithm to find the preimage of the new point, this paper uses a two-step Prediction-Correction scheme to find it.

The performance of the algorithm is tested by Hénon map. During the simulation, it is found that when $a = 1.4$, $b = 0.3$, the distribution of points of the unstable manifold is almost the same with that of Hénon map iteration sequence. The former is ordered while the latter is in chaos, it is to say, we obtain order out of chaos in Hénon map. And I didn't notice anyone else had ever gotten the same result. When some other groups of parameters are chosen, the unstable manifold behaves as the borderline of the direct Hénon map iteration sequence and the two branches of the manifold are symmetric in a certain sense, e.g. each branch of the unstable manifold in Figure 4 contains 9 folds. The unstable manifold in Figure 5 possesses a similar character.

Further exploration of the unstable manifold of Hénon map requires more work on experimenting different values of a and b, and we believe more beautiful pictures will come up to reveal the hidden properties of Hénon map. We hope our results be helpful to the further exploration of Hénon map.

References

[1] P Grassberger. On the fractal dimension of the Hénon attractor. *Phys. Lett. A*. 1983; 597(6): 224-226.
[2] HJ Gao, YS Zhang, SY Liang, DQ Li. A New chaotic algorithm for image encryption. *Chaos Solitons Fractals*. 2006; 29: 393–399.
[3] J Palis, WD Melo. Geometric Theory of Dynamical Systems. New York: Springer-Verlag. 1982.
[4] Z You, EJ Kostelich, JA Yorke. Calculating stable and unstable manifolds. *Int. J. Bifurc. Chaos Appl.Sci. Eng*., 1991; 1(3): 605–623.
[5] TS Parker, LO Chua. Practical Numerical Algorithms for Chaotic Systems. Berlin: Springer. 1989.
[6] D Hobson. An efficient method for computing invariant manifolds. *J. Comput. Phys.*, 1991; 104(1): 14-22.
[7] B Krauskopf, HM Osinga. Growing unstable manifolds of planar maps. 1517, 1997.

(http://www.ima.umn.edu/preprints/OCT97/1517.ps.gz.)
[8] B Krauskopf, HM Osinga. Growing 1D and quasi-2D unstable manifolds of maps. *J. Comput. Phys.* 1998; 146(1): 404–419.
[9] JP England, B Krauskopf, HM Osinga. Computing One-Dimensional Stable Manifolds and Stable Sets of Planar Maps without the Inverse. *SIAM J. Appl. Dyn. Syst.,* 2004; 3(2): 161-190.
[10] Khairudin. RBFNN Control of A Two-Link Flexible Manipulator Incorporating Payload. *TELKOMNIKA Indonesian Journal of Electrical Engineering.* 2010; 08(2): 157-164.
[11] P Srikanth, Ashwani Kumar Chandel. Inverse S-Transform Based Decision Tree for Power System Faults Identification. *TELKOMNIKA Indonesian Journal of Electrical Engineering.* 2011; 09(1): 99-106.